[6] A. R. Kerr and S.-K. Pan, "Some recent developments in the design of SIS mixers," *Int. J. Infrared Millim. Waves*, vol. 11, no. 10, pp. 1169–1187, Oct. 1990.
[7] H. Ogawa, A. Mizuno, M. Moko, H. Ishikawa, and Y. Fukui, "A 110 GHz SIS receiver for radio astronomy," *Int. J. Infrared Millim. Waves*, vol. 11, no. 6, pp. 717–726, June 1990.

Analysis of General Lossy Inhomogeneous and Anisotropic Waveguides by the Finite-Element Method (FEM) Using Edge Elements

Luis Nuño, Juan V. Balbastre, Héctor Castañé

***Abstract*—Several finite element formulations based on edge elements have been developed in recent years, avoiding the appearance of spurious modes in waveguides. However, no formulation of this kind dealing with general lossy inhomogeneous and anisotropic waveguides has been found in the literature. In this paper, a new finite element scheme for the most general linear waveguides has been derived from vector wave equations via a Galerkin procedure. In this formulation, triangular and quadrilateral edge elements have been used in order to avoid the spurious solutions. Furthermore, the final eigensystem involves only very sparse matrices, thus allowing important savings in time and memory.**

***Index Terms*— Anisotropic waveguides, edge elements, finite-element method.**

I. Introduction

The finite-element method (FEM) has been widely used in electromagnetics for the last two decades. Nevertheless, the earlier finite element analyses had the drawback of the appearance of spurious modes, leading to a considerable effort to avoid such nonphysical solutions [1]–[6].

More recently, two conditions have been found as requirements to avoid spurious solutions [7]: compatibility to guarantee the continuity of the tangential components of the fields and unisolvence to correctly model the curl operator null-space.

In the last years, several finite element formulations using vectorial interpolation have been developed [8]–[12]. Those vectorial elements satisfy both compatibility and unisolvence conditions so they do not present spurious modes. However, in the formulations of this kind found in the literature only lossless diagonal anisotropic waveguides have been considered. In this paper, the authors present a new edge element formulation valid for the most general lossy inhomogeneous and anisotropic linear waveguides.

First, a weak formulation of vector wave equations is obtained. This integral equation is valid for general anisotropic waveguides bounded by perfect electric or magnetic walls. Then, this integral equation is discretized following the FEM, obtaining a very sparse eigensystem where the eigenvalue is the propagation constant, attaining an important reduction in memory and central processing unit (CPU) time.

Manuscript received August 22, 1995; revised November 21, 1996. This work was supported by the Spanish CICYT, TIC95-0983-C03-02.

The authors are with the Departamento dé Comunicaciones, E.T.S.I. Telecomunicación de Valencia, Universidad Politécnica de Valencia, 46071, Valencia, Spain.

Publisher Item Identifier S 0018-9480(97)01718-3.

II. Weak Formulation

For the most general case of waveguides filled with lossy inhomogeneous and anisotropic materials, the problem is governed by the following vector wave equations:

$$\nabla \times (\hat{\mu}_r^{-1} \nabla \times \vec{E}) - k_0^2 \hat{\varepsilon}_r \vec{E} = 0$$
$$\nabla \times (\hat{\varepsilon}_r^{-1} \nabla \times \vec{H}) - k_0^2 \hat{\mu}_r \vec{H} = 0, \qquad k_0^2 = \omega^2 \varepsilon_0 \mu_0 \tag{1}$$

where $\hat{\varepsilon}_r$ and $\hat{\mu}_r$ are the relative electric permittivity and magnetic permeability tensors, respectively,

$$\hat{\varepsilon}_r = \begin{bmatrix} \varepsilon_{xx} & \varepsilon_{xy} & \varepsilon_{xz} \\ \varepsilon_{yx} & \varepsilon_{yy} & \varepsilon_{yz} \\ \varepsilon_{zx} & \varepsilon_{zy} & \varepsilon_{zz} \end{bmatrix}$$
$$\hat{\mu}_r = \begin{bmatrix} \mu_{xx} & \mu_{xy} & \mu_{xz} \\ \mu_{yx} & \mu_{yy} & \mu_{yz} \\ \mu_{zx} & \mu_{zy} & \mu_{zz} \end{bmatrix}. \tag{2}$$

The boundary conditions for electric or magnetic walls are, respectively,

$$\hat{n} \times \vec{E}|_C = 0$$

or

$$\hat{n} \times \vec{H}|_C = 0. \tag{3}$$

Assuming an exponential dependence of the fields with the z coordinate

$$\vec{E} = \vec{E}_0(x, y) e^{-\gamma z}$$
$$\vec{H} = \vec{H}_0(x, y) e^{-\gamma z}, \qquad \gamma = \alpha + j\beta \tag{4}$$

and defining the differential operators

$$D = \frac{\partial}{\partial x}\hat{x} + \frac{\partial}{\partial y}\hat{y} - \gamma \hat{z}$$
$$\overline{D} = \frac{\partial}{\partial x}\hat{x} + \frac{\partial}{\partial y}\hat{y} + \gamma \hat{z} \tag{5}$$

leads to very elegant and compact expressions after applying the Galerkin procedure to the waveguide section S:

$$\iint_S (\overline{D} \times \vec{F}_0) \cdot (\hat{\mu}_r^{-1} D \times \vec{E}_0)\, dS - k_0^2 \iint_S \vec{F}_0 \cdot (\hat{\varepsilon}_r \vec{E}_0)\, dS = 0 \tag{6a}$$

$$\iint_S (\overline{D} \times \vec{G}_0) \cdot (\hat{\varepsilon}_r^{-1} D \times \vec{H}_0)\, dS - k_0^2 \iint_S \vec{G}_0 \cdot (\hat{\mu}_r \vec{H}_0)\, dS = 0 \tag{6b}$$

with $\vec{F}_0$ and $\vec{G}_0$ being the test functions, which satisfy the same boundary conditions as $\vec{E}_0$ and $\vec{H}_0$, respectively.

III. Finite Element Scheme

Because of the dual form of (6), only the finite element scheme for the electric field derived from (6a) will be presented. The transversal components of $\vec{E}_0$ and $\vec{F}_0$ will be interpolated with the first-order vector edge functions while their axial components will be

interpolated with the first-order Lagrange nodal functions in order to avoid spurious solutions:

$$\vec{E}_0 = \begin{bmatrix} U^T & 0 \\ V^T & 0 \\ 0 & N^T \end{bmatrix} \begin{bmatrix} \dot{E}_t \\ \dot{E}_z \end{bmatrix} = P^T \dot{E}$$
$$\vec{F}_0 = \begin{bmatrix} U^T & 0 \\ V^T & 0 \\ 0 & N^T \end{bmatrix} \begin{bmatrix} \dot{F}_t \\ \dot{F}_z \end{bmatrix} = P^T \dot{F} \tag{7}$$

where the dots indicate the values of the functions at edges or nodes and the expressions for the interpolating functions U, V, and N can be found in many sources (see [9]). So, the differential operations involved in (6a) give

$$D \times \vec{E}_0 = \begin{bmatrix} \gamma V^T & N_y^T \\ -\gamma U^T & -N_x^T \\ V_x^T - U_y^T & 0 \end{bmatrix} \begin{bmatrix} \dot{E}_t \\ \dot{E}_z \end{bmatrix} = Q^T \dot{E}$$
$$\overline{D} \times \vec{F}_0 = \begin{bmatrix} -\gamma V^T & N_y^T \\ \gamma U^T & -N_x^T \\ V_x^T - U_y^T & 0 \end{bmatrix} \begin{bmatrix} \dot{F}_t \\ \dot{F}_z \end{bmatrix} = \overline{Q}^T \dot{F} \tag{8}$$

with the subindices x and y in the interpolating functions standing for differentiation with respect to these variables. After some algebraic manipulations the following eigensystem is obtained:

$$\begin{bmatrix} \gamma^2 M_1 + \gamma M_2 + M_3 & \gamma M_4 + M_5 \\ \gamma M_6 + M_7 & M_8 \end{bmatrix} \dot{E} - k_0^2 \begin{bmatrix} N_1 & N_2 \\ N_3 & N_4 \end{bmatrix} \dot{E} = 0 \tag{9}$$

where the submatrices involve integrals of the interpolating functions and their derivatives (see the Appendix) and the size of the eigensystem is reduced by introducing the boundary conditions. On the other hand, this eigensystem can be transformed in such a way that γ becomes the eigenvalue

$$\gamma^2 \begin{bmatrix} M_1 & 0 \\ 0 & 0 \end{bmatrix} \dot{E} + \gamma \begin{bmatrix} M_2 & M_4 \\ M_6 & 0 \end{bmatrix} \dot{E} + \begin{bmatrix} M_3 - k_0^2 N_1 & M_5 - k_0^2 N_2 \\ M_7 - k_0^2 N_3 & M_8 - k_0^2 N_4 \end{bmatrix} \dot{E} = 0. \tag{10}$$

It is interesting to point out that these eigensystems are completely free of spurious solutions and the matrices involved are highly sparse, thus allowing a great memory and time reduction. The transformation of (10) into a generalized sparse eigensystem can be achieved simply by introducing $\lambda = 1/\gamma$, $\overline{E}_t = \dot{E}_t/\lambda$:

$$\lambda \begin{bmatrix} M_3 - k_0^2 N_1 & M_5 - k_0^2 N_2 & 0 \\ M_7 - k_0^2 N_3 & M_8 - k_0^2 N_4 & 0 \\ 0 & 0 & I \end{bmatrix} \begin{bmatrix} \dot{E}_t \\ \dot{E}_z \\ \overline{E}_t \end{bmatrix} + \begin{bmatrix} M_2 & M_4 & M_1 \\ M_6 & 0 & 0 \\ -I & 0 & 0 \end{bmatrix} \begin{bmatrix} \dot{E}_t \\ \dot{E}_z \\ \overline{E}_t \end{bmatrix} = 0 \tag{11}$$

where it is necessary to ignore as many eigenvalues $\lambda = 0$ as $\dot{E}_z$ has unknowns, corresponding to the nonvalid solutions

$$\dot{E}_t = 0$$
$$\overline{E}_t = -M_1^{-1} M_4 \dot{E}_z \tag{12}$$

introduced in the transformation process. These nonvalid solutions must not be confused with any kind of spurious modes since their origin is an algebraic transformation for reducing the order of an eigensystem, being perfectly defined and located.

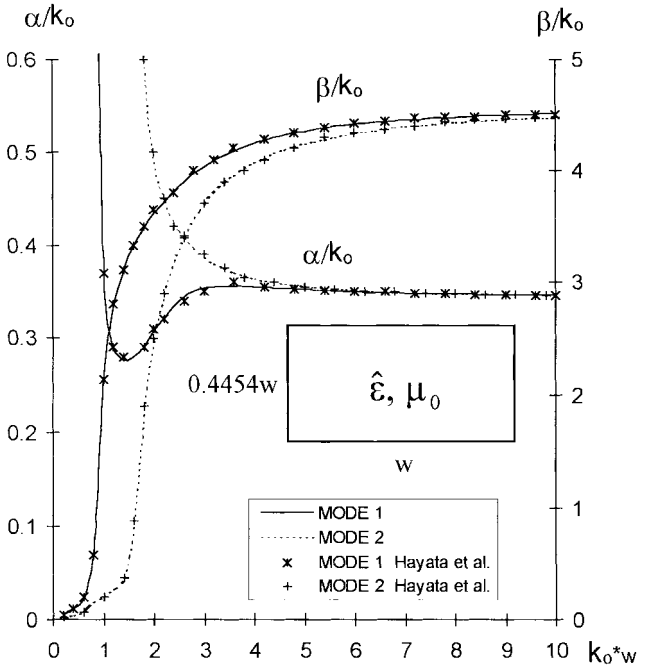

Fig. 1. Rectangular anisotropic homogeneous waveguide.

IV. Numerical Results

In this section, numerical results of several anisotropic waveguides are presented, using first-order triangular and quadrilateral elements. First, a rectangular waveguide is considered (see Fig. 1), filled with

$$\hat{\varepsilon} = \begin{bmatrix} 18.5875 - j2.57 & -3.8841 + j1.0219 & 0 \\ -3.8841 + j1.0219 & 14.1025 - j1.39 & 0 \\ 0 & 0 & 11.86 - j0.80 \end{bmatrix} \varepsilon_0$$

The propagation characteristics of the first two modes, obtained using an eigensystem of size $N = 440$, agree very well with those presented in [1].

Next, the shielded microstrip line of Fig. 2 has been analyzed, with the substrate $\varepsilon_x = \varepsilon_z = 9.4\varepsilon_0$, $\varepsilon_y = 11.6\varepsilon_0$, and $N = 275$ unknowns. The propagation constant of the first two modes are represented and compared with [9], showing a very good agreement.

Afterwards, the ferrite-loaded waveguide of Fig. 3 was solved with $N = 560$ and compared with [4], with both results being seen as very similar. The ferrite slab characteristics were

$$\varepsilon = 10\varepsilon_0$$
$$\hat{\mu} = \begin{bmatrix} 0.875 & 0 & -j0.375 \\ 0 & 1 & 0 \\ j0.375 & 0 & 0.875 \end{bmatrix} \mu_0.$$

As an example of curvilinear boundaries, the propagation constant of the first three modes has been computed for the elliptical waveguide of Fig. 4, the first two modes being compared with [4]. The electromagnetic properties of the materials were

$$\varepsilon_1 = 10\varepsilon_0$$
$$\hat{\mu}_1 = \begin{bmatrix} 0.875 & 0 & -j0.375 \\ 0 & 1 & 0 \\ j0.375 & 0 & 0.875 \end{bmatrix} \mu_0$$
$$\hat{\varepsilon}_2 = \begin{bmatrix} 2.25 & 0 & 0 \\ 0 & 2.25 & 0 \\ 0 & 0 & 1.5 \end{bmatrix} \varepsilon_0$$
$$\mu_2 = \mu_0.$$

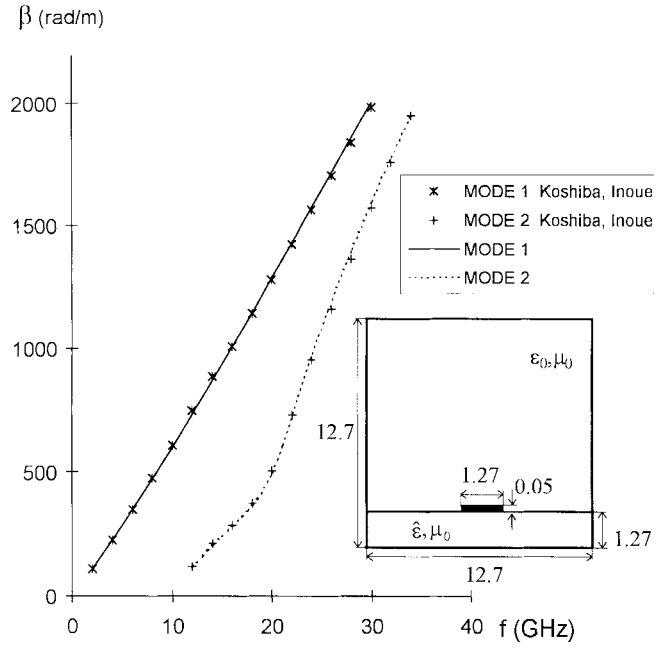

Fig. 2. Anisotropic shielded microstrip (dimensions in millimeters).

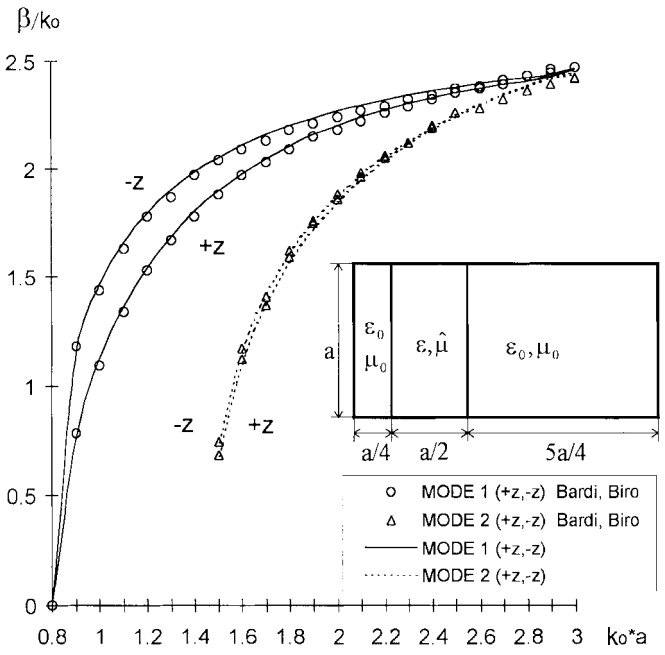

Fig. 3. Ferrite-loaded rectangular waveguide.

Finally, to provide a very general example, the authors have analyzed a trapezoidal microstrip line with three anisotropic materials. The propagation characteristics are shown in Fig. 5(a) and the transversal components of the electric and magnetic fields for the second mode are plotted in Fig. 5(b). The materials 1 and 2 in the waveguide are the same as in the previous example, while $\varepsilon_{3x} = \varepsilon_{3z} = (11.86 - j0.375)\varepsilon_0, \varepsilon_{3y} = (20.83 - j3.16)\varepsilon_0, \mu_3 = \mu_0$.

V. Conclusion

Analysis of general lossy inhomogeneous and anisotropic waveguides has been carried out by the FEM using vector basis functions for the transversal components of the fields to avoid spurious solutions,

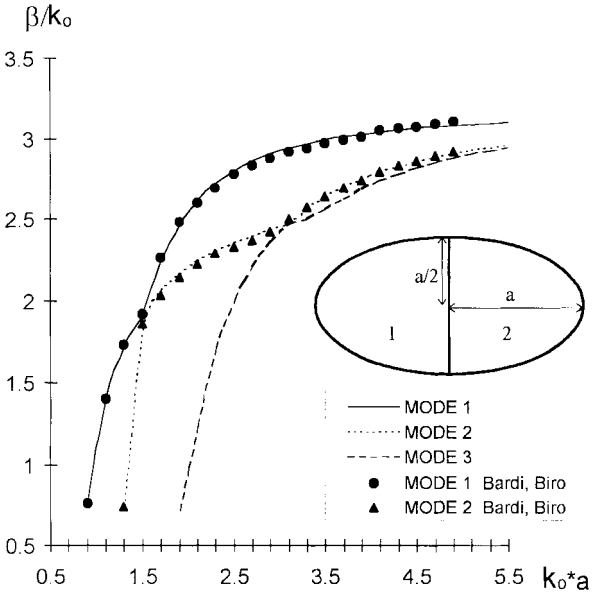

Fig. 4. Elliptical waveguide filled with two anisotropic materials.

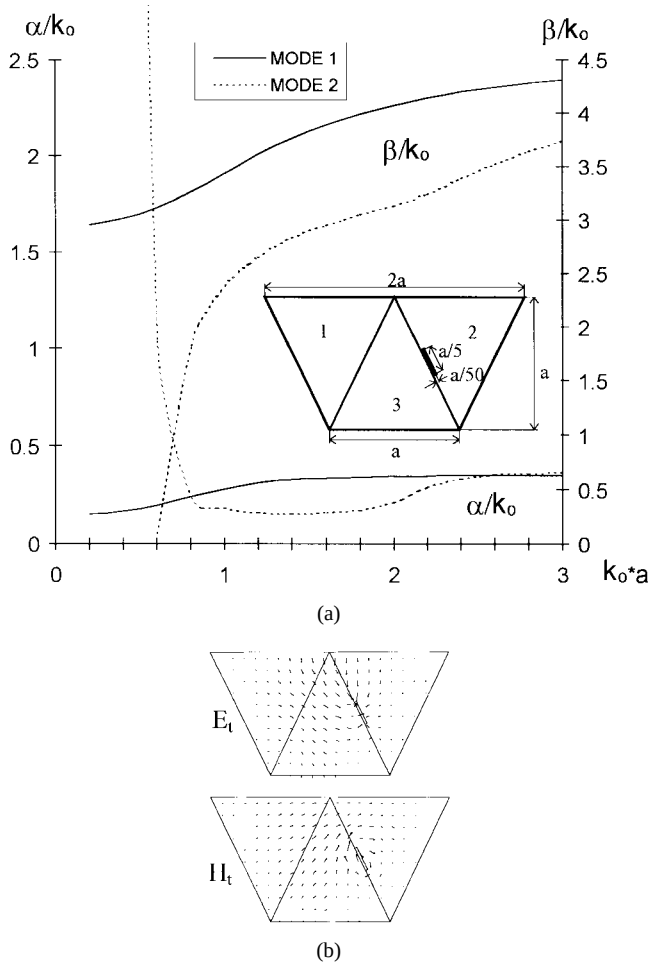

Fig. 5. Anisotropic and inhomogeneous trapezoidal microstrip line: (a) geometry and propagation constants and (b) transversal electric and magnetic fields for the second mode.

with their axial components being interpolated with Lagrange nodal basis functions. The matrices involved in the final eigensystem are ex-

tremely sparse, thus allowing a very high time and memory efficiency. The number of examples presented show a very good agreement with previous studies and guarantee the general applicability of the method. Finally, the last example is intended to serve as a reference for later analyses.

APPENDIX

Definition of the submatrices involved in (9):

$$M_1 = \iint_S (-VW_{x1}^T + UW_{y1}^T)\,dS \tag{A1}$$

$$M_2 = \iint_S [-VW_{x2}^T + UW_{y2}^T + (V_x - U_y)W_{z1}^T]\,dS \tag{A2}$$

$$M_3 = \iint_S (V_x - U_y)W_{z2}^T\,dS \tag{A3}$$

$$M_4 = \iint_S (-VW_{x3}^T + UW_{y3}^T)\,dS \tag{A4}$$

$$M_5 = \iint_S (V_x - U_y)W_{z3}^T\,dS \tag{A5}$$

$$M_6 = \iint_S (N_yW_{x1}^T - N_xW_{y1}^T)\,dS \tag{A6}$$

$$M_7 = \iint_S (N_yW_{x2}^T - N_xW_{y2}^T)\,dS \tag{A7}$$

$$M_8 = \iint_S (N_yW_{x3}^T - N_xW_{y3}^T)\,dS \tag{A8}$$

where

$$W_{x1}^T = (\hat{\mu}^{-1})_{xx}V^T - (\hat{\mu}^{-1})_{xy}U^T \tag{A9}$$

$$W_{y1}^T = (\hat{\mu}^{-1})_{yx}V^T - (\hat{\mu}^{-1})_{yy}U^T \tag{A10}$$

$$W_{z1}^T = (\hat{\mu}^{-1})_{zx}V^T - (\hat{\mu}^{-1})_{zy}U^T \tag{A11}$$

$$W_{x2}^T = (\hat{\mu}^{-1})_{xz}(V_x^T - U_y^T) \tag{A12}$$

$$W_{y2}^T = (\hat{\mu}^{-1})_{yz}(V_x^T - U_y^T) \tag{A13}$$

$$W_{z2}^T = (\hat{\mu}^{-1})_{zz}(V_x^T - U_y^T) \tag{A14}$$

$$W_{x3}^T = (\hat{\mu}^{-1})_{xx}N_y^T - (\hat{\mu}^{-1})_{xy}N_x^T \tag{A15}$$

$$W_{y3}^T = (\hat{\mu}^{-1})_{yx}N_y^T - (\hat{\mu}^{-1})_{yy}N_x^T \tag{A16}$$

$$W_{z3}^T = (\hat{\mu}^{-1})_{zx}N_y^T - (\hat{\mu}^{-1})_{zy}N_x^T. \tag{A17}$$

Finally,

$$N_1 = \iint_S [U(\varepsilon_{xx}U^T + \varepsilon_{xy}V^T) + V(\varepsilon_{yx}U^T + \varepsilon_{yy}V^T)]\,dS \tag{A18}$$

$$N_2 = \iint_S (\varepsilon_{xz}UN^T + \varepsilon_{yz}VN^T)\,dS \tag{A19}$$

$$N_3 = \iint_S N(\varepsilon_{zx}U^T + \varepsilon_{zy}V^T)\,dS \tag{A20}$$

$$N_4 = \iint_S \varepsilon_{zz}NN^T\,dS. \tag{A21}$$

REFERENCES

[1] K. Hayata, K. Miura, and M. Koshiba, "Full vectorial finite element formalism for lossy anisotropic waveguides," *IEEE Trans. Microwave Theory Tech.*, vol. 37, pp. 875–883, May 1989.

[2] K. D. Paulsen and D. R. Lynch, "Elimination of vector parasites in finite element Maxwell solutions," *IEEE Trans. Microwave Theory Tech.*, vol. 39, pp. 395–404, Mar. 1991.

[3] R. Miniowitz and J. P. Webb, "Covariant-projection quadrilateral elements for the analysis of waveguides with sharp edges," *IEEE Trans. Microwave Theory Tech.*, vol. 39, pp. 501–505, Mar. 1991.

[4] I. Bardi and O. Biro, "An efficient finite-element formulation without spurious modes for anisotropic waveguides," *IEEE Trans. Microwave Theory Tech.*, vol. 39, pp. 1133–1139, July 1991.

[5] Y. Lu and F. A. Fernandez, "An efficient finite element solution of inhomogeneous anisotropic and lossy dielectric waveguides," *IEEE Trans. Microwave Theory Tech.*, vol. 41, pp. 1215–1223, June/July 1993.

[6] L. Nuño, J. V. Balbastre, J. Igual, M. Ramón and M. Ferrando, "Analysis of inhomogeneous and anisotropic waveguides by the finite element method," in *2nd Topical Mtg. Elect. Performance Electron. Packaging*, Monterey, CA, Oct. 20–22, 1993, pp. 47–49.

[7] Z. J. Cendes, "Vector finite elements for electromagnetic field computation," *IEEE Trans. Magn.*, vol. 27, pp. 3958–3966, Sept. 1991.

[8] J. F. Lee, D. K. Sun, and Z. J. Cendes, "Tangential vector finite elements for electromagnetic field computation," *IEEE Trans. Magn.*, vol. 27, pp. 4032–4035, Sept. 1991.

[9] M. Koshiba and K. Inoue, "Simple and efficient finite-element analysis of microwave and optical waveguides," *IEEE Trans. Microwave Theory Tech.*, vol. 40, pp. 371–377, Feb. 1992.

[10] B. M. Dillon and J. P. Webb, "A comparison of formulations for the vector finite element analysis of waveguides," *IEEE Trans. Microwave Theory Tech.*, vol. 42, pp. 308–316, Feb. 1994.

[11] Y. Lu and F. A. Fernandez, "Vector finite element analysis of integrated optical waveguides," *IEEE Trans. Magn.*, vol. 30, pp. 3116–3119, Sept. 1994.

[12] B. C. Anderson and Z. J. Cendes, "Solution of ferrite loaded waveguide using vector finite elements," *IEEE Trans. Magn.*, vol. 31, pp. 1578–1581, May 1995.

Some Characteristics of Ridge-Trough Waveguide

Debatosh Guha and Pradip Kumar Saha

***Abstract*—A single-ridged waveguide with a symmetrical longitudinal trough below the ridge, designated as a ridge-trough waveguide (RTW) has been recently proposed as a wafer probe. The authors have theoretically calculated the cutoff, bandwidth, and impedance characteristics of this modified single-ridged waveguide in two different configurations using the Ritz–Galerkin technique and different domain decompositions. The results indicate that a RTW can be a low impedance broad-band structure.**

***Index Terms*—Low impedance broad-band waveguide.**

I. INTRODUCTION

In recent years microwave researchers have been paying attention to developing transitions between the coplanar waveguide (CPW) and other microwave transmission media for efficient utilization of some of the advantages of the CPW (one of which is its suitability in the design of microwave wafer probes [1]). A few rectangular waveguides to CPW transitions have been reported which utilize finline transitions [2], [3], modified ridged waveguides [4], [5], and some other configurations [6], [7].

Of these structures, the ridge-trough waveguide (RTW) [5] has attracted the authors' attention, prompting them to analyze rectangular waveguides with ridges and shaped septa which promise broad-

Manuscript received August 22, 1995; revised November 21, 1996.

The authors are with the Institute of Radio Physics and Electronics, University of Calcutta, 700 009 Calcutta, India.

Publisher Item Identifier S 0018-9480(97)01714-6.